Entropy change and kinetic effects at the magnetostructural phase transition of MnBi

Entropy change and kinetic effects at the magnetostructural phase transition of MnBi

Vittorio Basso, Elena Sonia Olivetti, Luca Martino, Michaela Küpferling

Istituto Nazionale di Ricerca Metrologica, Strada delle Cacce 91, 10135 Torino, Italy

Abstract

In this paper we investigate the entropy change and the kinetics at the magneto-structural transition (at 628 K) of polycrystalline MnBi. Samples were prepared by rapid quenching and annealing and exhibit 86 wt% of the hexagonal MnBi phase. The entropy change at the transition is found to be Δs =17.6 $\mathrm{Jkg^{-1}K^{-1}}$ and the magnetic field shifts the transition temperature at a rate of 2.6 $\mathrm{KT^{-1}}$. The temperature hysteresis, of 19 K, is quite large for magneto-thermal application. The transition shows kinetics effects upon cooling in which the transition temperature is found to depend approximately to the logarithm of the temperature rate with coefficient -3.8 K.

Key words: magnetocaloric effect, MnBi, first order phase transition, kinetic effects

NOMENCLATURE

s - specific entropy

s_{PM} - specific entropy in the paramagnetic state

Δs - isothermal entropy change (specific)

T - absolute temperature

ΔT_{ad} - adiabatic temperature change

T_s - sample temperature

H - applied magnetic field

M - magnetization

μ_0 - permeability of vacuum

q_s - heat flux

R - thermal contact resistance

m_s - sample mass

c_p - specific heat capacity

1 Introduction

MnBi is a ferromagnet with saturation magnetization of 0.82 T (74.7 $\mathrm{Am^2kg^{-1}}$) at 300 K. It has been extensively investigated in the past for its high anisotropy value $\mu_0 H_{AN} = 2.2 \cdot 10^6$ $\mathrm{Jm^{-3}}$ at 500 K and for its high Kerr rotation (Chen and Stutius, 1974; Yin et al., 1996; Yang et al., 2002). It also displays a magnetostructural transition at 628 K and a spin reorientation transition at 84 K (Coey, 2009). At the magnetostructural transition the material transforms from the low temperature ferromagnetic α-phase to the high temperature paramagnetic β phase. The α-MnBi has the hexagonal NiAs-type crystal structure with the Bi atoms forming an hcp sublattice and Mn atoms filling all the octahedral holes formed by the Bi sublattice. The cell parameters are a=4.29 Å and c=6.13 Å. The β-MnBi has an a-axis dilatation (+1.2%, a=4.34 Å) and a c-axis contraction (-2.5%, c=5.97 Å) with almost no volume change with

respect to the low temperature phase. A small lattice distortion in the basal plane occurs during the transformation and the crystal symmetry is slightly changed from hexagonal to orthorhombic. The $\alpha \rightarrow \beta$ transition is also accompanied by Mn diffusion. It was estimated that in the β-phase about 15% of the Mn atoms have left their initial octahedral sites to fill the trigonal bipyramidal holes (Heikes, 1955; Roberts, 1956; Andersen et al., 1967). The β-phase can be stabilized at room temperature by quenching. As the β-phase is characterized by the bipyramidal holes available for Mn, it can also host excess Mn. By proper annealing at temperatures above 628K it is possible to form the off-stoichiometric $Mn_{1+x}Bi$ compound, which is between the NiAs-type structure of the α-MnBi, with the Mn only in the octahedral holes, and the Ni_2In-type structure, in which both the octahedral and the bipyramidal holes are filled. After a quench, the β-phase can retain up to a maximum x=0.08 of Mn (Chen and Stutius, 1974; Yin et al., 1996) while the rest separates as pure Mn. The quenched β-phase is also ferromagnetic with a Curie point around 430 K. In this paper we have investigated the entropy change and the kinetics of the magnetostructural $\alpha - \beta$ phase transition.

2 Sample preparation and analysis

Polycrystalline samples were prepared by following the standard method of Ref.(Chen and Stutius, 1974). i) The 50 at% Mn and 50 at% Bi master alloy was prepared by induction melting in vacuum of high purity elements. ii) The alloy was remelted in vacuum and quenched into a water cooled Cu mold of 5mm diameter in order to promote phase homogenization and small grain size. iii) The samples were annealed in vacuum at 608 K for 1 hour to pro-

mote the growth of the MnBi with respect to Bi and Mn phases (Basso et al., 2012a). The sample microstructure and elemental composition were analyzed on polished specimens by means of Scanning Electron Microscopy (SEM) coupled with Energy Dispersive Spectroscopy (EDS) after each of the steps. Phase identification was accomplished by means of X-ray diffraction (XRD) in Bragg-Brentano configuration with the Co Kα radiation. Phase transitions have been studied by power compensation differential scannig calorimetry (DSC).

The master alloy revealed a partial loss in Bi atoms occurred during alloy melting due to the high vapor pressure of this metal. The quenching has the effect of reducing the typical grain size from the order of 100 μm to that of 10 μm, but the alloy still contains a considerable presence of unreacted Mn and Bi. The overall elemental composition is 58 at% Mn and 42 at% Bi. After annealing, the sample has a fairly uniform morphology consisting of a predominant $Mn_{50}Bi_{50}$ phase together with pure Mn crystals (average diameter < 5 μm) and the occasional presence of a residual Bi-rich intergranular phase (Fig. 1). The diffraction pattern confirmed the presence of the hexagonal NiAs-type structure of α-MnBi, together with small amounts of residual rhombohedral Bi and pure cubic Mn (Fig.2).

The phase fraction of the Bi-rich phase was determined by taking the ratio of the latent heat measured on the multi-phase sample at the temperature of 537 K ($2.6{\cdot}10^3$ Jkg^{-1}) with the latent heat of melting of Bi ($54.1 \cdot 10^3$ Jkg^{-1}). This estimate gives 5 wt% ($\sim$ 3 at%). Considering the average atomic composition (Mn 58 at%, Bi 42 at%), the phase fraction of the MnBi phase in the sample results to be 86 wt% (78 at%) and Mn is the remaining 9 wt% ($\sim$19 at%).

3 Magneto-thermal behavior

The thermal behavior of the studied sample has been analyzed upon both heating and cooling during a constant temperature rate DSC scan. Typical DSC traces are displayed in figure 3. Two endothermic events are recorded upon heating: the Bi-rich phase has a melting point close to MnBi eutectic at 537 K (the melting point of Bi is 544 K) and the α-β transformation of MnBi is found at 628 K. The latent heat measured at the $\alpha \rightarrow \beta$ transition is $10.4{\cdot}10^3$ Jkg^{-1}. On cooling we find the $\beta \rightarrow \alpha$ transition at 609 K and the Bi-rich phase solidification at 501 K (Fig.3). To determine the entropy change at the transition, we computed the $s(T_s)$ curve by the integration of the measured heat flux from DSC. The entropy is given by

$$s(T_s) - s_0 = \frac{1}{m_s} \int_0^t \frac{q_s}{T_s} dt \tag{1}$$

where q_s is the heat flux to the sample, and T_s is the sample temperature. T_s as a function of time t is computed from the measured temperature T by taking into account the presence of a thermal contact resistance R between the sample and the thermometer $T_s = T - Rq_s$ where R depends on the contact area A and the quality of the contact of the sample with the sample pan. The value of R was determined by the coincidence of the melting point of the Bi-rich phase in scans performed at different temperature rates (2.5, 5, 10 Kmin^{-1}). Typically we find $1/(RA) \sim 1 \cdot 10^3$ WK^{-1}m^{-2}. The resulting sample entropy is shown in Fig.4. The specific heat $c_p = Tds/dT$ is approximately constant $c_p = 220$ Jkg^{-1}K^{-1} above the transition, at $T > 630$ K, and well below it, at $T < 500$ K. This value can be compared with 208 Jkg^{-1}K^{-1}, the limit given by the specific heat at constant volume of the Dulong-Petit law $c_v = 3k_B N_A/m$, where k_B is

the Boltzmann constant, N_A the Avogadro number and m the average atomic mass of the alloy. From the comparison we deduce that the main contribution comes from the lattice, whereas the contributions from the thermal expansion and from the electronic degrees of freedom are relatively small. Just below the transition, the specific heat is larger than the base value of 220 $\mathrm{Jkg^{-1}K^{-1}}$. This difference can be attributed to the contribution of the magnetic spin system which is relevant in the vicinity of the phase transitions. The measured thermal hysteresis loop is strongly asymmetric showing a long open tip down to 550 K with different values of c_p (see dotted lines of Fig.4). The entropy change at the transition is evaluated with the help of the extrapolation of the dotted lines in Fig.4: we find Δs=17.6 $\mathrm{Jkg^{-1}K^{-1}}$ on heating and Δs =14.0 $\mathrm{Jkg^{-1}K^{-1}}$ on cooling.

Magnetic measurements were performed by vibrating sample magnetometer (VSM) from room temperature (296 K) up to 650 K under different constant magnetic fields (Fig.5). Temperature was changed at the rate of 0.027 $\mathrm{Ks^{-1}}$ (1.6 K/min). At room temperature and 1.2 T the magnetization is 70 $\mathrm{Am^2kg^{-1}}$. On heating the transition occurs at 627 K, where the magnetization of the ferromagnetic α-phase is 40.5 $\mathrm{Am^2kg^{-1}}$. Above the transition, when the β-phase is formed, the behavior is paramagnetic and follows approximately a Curie law with a magnetic moment of 4.3 μ_B per Mn atom (Basso et al., 2012a; Andersen et al., 1967; Chen and Stutius, 1974; Yang et al., 2002). Upon cooling the transition to the ferromagnetic state occurs in two steps: i) the first one is a steep jump around 609 K in which the magnetization increases up to 35.5 $\mathrm{Am^2kg^{-1}}$, i.e. the 80% of the corresponding value measured on heating (43.2 $\mathrm{Am^2kg^{-1}}$); ii) the second step is a smooth transition in which the magnetization curve upon cooling rejoins the heating one at about 560 K. The

behavior is analogous to that found in the entropy curve (Fig.5). This two-step transition was not previously noted in the literature. A possible interpretation of this effect is given in section 4. The dependence of the transition temperatures (T_t) on the applied magnetic field, was studied on both heating and cooling by considering the steep changes and fitting the magnetization curves by the function $\Delta M(1+\tanh((T-T_t)/T_0))/2$. The values of T_t are shown in Fig.6 while T_0 is 0.8 K on heating and 1.8 K on cooling. The transition on heating shifts of 2.6 KT^{-1} while on cooling of 2.8 KT^{-1}. By computing the right hand side of the Clausius-Clapeyron equation

$$\frac{1}{\mu_0}\frac{\partial T}{\partial H} = -\frac{\Delta M}{\Delta s} \tag{2}$$

we obtain 2.3 KT^{-1} on heating and 2.5 KT^{-1} on cooling. The difference is of the order of 10% and can be attributed to the fact that the magnetization change ΔM, evaluated by the change at the magnetic field of 1.2 T, is an underestimation of the saturation magnetization change, while the extrapolation method used for Δs may lead to an overestimation.

The magnetic field induced entropy change has been determined from measured magnetization curves through the integration of the Maxwell relation

$$\frac{1}{\mu_0}\frac{\partial s}{\partial H} = \frac{\partial M}{\partial T} \tag{3}$$

giving

$$s(H,T) - s(0,T) = \frac{\partial}{\partial T}\left[\int_0^H \mu_0 M dH\right] \tag{4}$$

The result is shown in Fig.7. The two peaks of heating and cooling are placed at well separated temperatures because of the presence of a large tempera-

ture hysteresis in the phase transformation (19 K). This separation of the peaks means that the magnetocaloric effect is largely irreversible (Basso et al., 2012b).

The kinetics of the first order phase transformation was investigated by changing the temperature scan rate of DSC from 0.5 to 40 K/min. The result is shown in Fig. 8 as the entropy $s(T_s)$ curve obtained by Eq. (1). It is found that the transition temperature depends on the rate only upon cooling. This experimental fact was already noted in Ref. (Andersen et al., 1967) but never quantified before. The transition upon cooling depends approximatively linearly on the logarithm of the rate. It can be deduced that the underlying phenomena are related to the thermal activation over energy barriers (Basso et al., 2000).

4 Discussion

The phenomenology of the entropy change of MnBi is similar to the one of the Heusler alloys with large temperature hysteresis in which the magnetocaloric effect depends on the time history of the magnetic field and temperature. In MnBi, with a temperature hysteresis of 19 K, the entropy change of Fig.7 is irreversible: it can be observed only by the T, H sequence in which the magnetic field change produces the same effect of the previous temperature change. In our case it is the heating with magnetic field followed by its removal (Basso et al., 2012b). To fully characterize the magnetocaloric effect at the first order transition of MnBi polycrystal we computed the entropy diagram $s(H, T)$. To do this, we have combined magnetic and thermal data using Eq.(4) with the first term, $s(0, T)$, given by the DSC thermal measurement and the

second term by the magnetic measurement. With the data taken on the same specimen, we obtain the plot of Fig.9, where only the heating branches are shown. From Fig.9 we can compute the adiabatic temperature change. With a magnetic field of 1.2 T the temperature change at 628.5 K is $\Delta T_{ad} = 2.5$ K. For MnBi, due to the particularly low value of the specific heat, the maximum allowed adiabatic temperature change may be rather large and may eventually overcome the hysteresis width. To make such an estimate, we do a linear extrapolation of the $ds/dT = 0.44$ Jkg^{-1}K^{-2} measured in the ferromagnetic state, to higher temperatures. The maximum allowed adiabatic temperature change is then $\Delta T_{ad(max)} = \Delta s/(ds/dT) \sim 37$ K. By taking the experimental transition temperature shift of 2.6 KT^{-1}, to obtain the maximum value one needs a rather large value of 14 T.

The results obtained so far indicate that MnBi has a too large hysteresis to be used as magnetocaloric heat pump with the magnetic fields of permanent magnets (< 2 T), however from our study some interesting characteristics of the physics of its phase transition emerge. These are summarized as follows. i) We have obtained an estimate of the entropy change of MnBi at the $\alpha - \beta$ transition. The measured entropy change, if ascribed to the MnBi phase fraction, gives 20.5 Jkg^{-1}K^{-1}. This value attributed to Mn atoms, corresponds to a change of 0.65 $N_A k_B$. By considering the mean field theory with S=4/2, the magnetic entropy change corresponding to a magnetization change M/M_s from 0.5 to 0 is only $\sim 0.3 N_A k_B$. Then the measured entropy change should originate in part also from the lattice, as pointed out also by Hubermann and Streifer (Hubermann and Streifer, 1975) who studied the thermodynamics of MnBi with some Mn atoms in the interstices. In this sense the behavior of MnBi is opposite with respect to MnAs in which the lattice entropy change is

negative at the transition because of an a-axis contraction around 1.1% (Bean and Rodbell, 1962). ii) The particular asymmetric shape of the hysteresis with two steps upon cooling is a peculiar fact that needs further experimental investigation. A tentative interpretation of this effect is the following. As a preliminary comment it has to be noticed that it is known from the literature that at the first order transition there is a diffusion of around 15% of Mn from octahedral sites to the trigonal bipyramidal sites, when the c/a decrease (see an illustration in Fig.10). Upon heating this creates a disordered configuration for the Mn atoms (random holes in the octahedral sites and random filling in the bipyramidal sites). Upon cooling the ordered configuration needs to be recreated. The need to arrive to an ordered situation may corresponds to an extra energy barrier, additional to atomic diffusion. Yin et al. (Yin et al., 1996) have argued that the out-of-equilibrium formation of the α-phase may pass through an intermediate disordered phase in which either Mn or Bi may provisionally fill the empty octahedral sites. Similarly, for our case, it may be possible that the $\beta \rightarrow \alpha$ transition upon cooling occurs through two stages: first, the diffusion of both Mn or Bi into the empty octahedral holes, recreating a disordered intermediate version of the NiAs-type structure; second, the ordering of the Mn and Bi at their equilibrium ordered positions. This second process may be characterized by a higher energy barrier and may be related to the increase of the hysteresis width in the tail upon cooling. Further investigation will be devoted to understand this last point. iii) A kinetic effect in the phase transformation in the first step of the transition is found upon cooling. The kinetics is seen as a linear dependence of the transition temperature on the logarithm of the temperature rate. This kind of behavior is the one that is typically found in systems with two energy minima separated by an energy barrier. The effect of the decreasing temperature is that of stabilizing

the low temperature minimum, while at the same time the thermal activation helps to overcome the barrier before the critical instability. When the system is driven slowly the transition occurs then at a higher temperature. In thermal activation models it is possible to connect the slope with the typical volume that is coherently transformed by the help of thermal fluctuation. In Fig.8 the change of the transition temperature with the logarithm of the rate has absolute value $T^* = 3.8$ K. In analogy with the magnetic case (Basso et al., 2000) we use the formula $T^* = k_B T/(\Delta s\, v_0)$, where Δs is the entropy change at the transition (in volume density), and we derive the activation volume v_0. The resulting volume has linear size $v_0^{1/3}$ around 12 Å. This means that the activation volume is composed by around 120 atoms. Going back to the physical interpretation we observe that the phenomenology found is coherent with the picture described just before. While upon heating each atom can diffuse independently and with negligible energy barriers into the empty holes, upon cooling this is no more possible. The recreation of the α phase has to pass by the refilling of all the empty NiAs-type sites.The cooling process cannot be thought as the sum of individual and independent atomic diffusion events, but as a process that requires the coordinated diffusion of a number of atoms. If we consider that 15% of Mn left their sites, from the volume that we have derived, the typical number of atoms participating to this coordinated back diffusion is of the order of 10. To verify this interpretation it would be interesting to test the atomic positioning of Mn and Bi in the quenched alloys. In fact this picture of the phase transition in two steps, predicts the existence of both a quenched disordered β phase (when quenching occurs from above 628 K) and a quenched disordered α phase (when quenching occurs from the range between 560 K and 610 K). Future investigations will be dedicated to clarify this point.

5 Conclusions

We have performed an experimental investigation on the magnetocaloric properties of MnBi at its magneto-structural phase transition at 628 K. Polycrystalline samples have been prepared by rapid quenching and structurally characterized, resulting in a 86 wt% of the hexagonal MnBi phase. The entropy change at the transition is found to be Δs =17.6 Jkg^{-1}K^{-1} and the magnetic field shifts the transition temperature of 2.6 KT^{-1}. The magneto-structural phase transition has a temperature hysteresis of 19 K which is quite large to achieve a reversible magneto-thermal effect. However, due to the particularly low value of the specific heat, the maximum allowed adiabatic temperature change may be rather large and may eventually overcome the hysteresis width. With $ds/dT = 0.44$ Jkg^{-1}K^{-2} measured in the ferromagnetic state, the maximum allowed adiabatic temperature change is $\Delta T_{ad(max)} = \Delta s/(ds/dT)$ giving $\Delta T_{ad(max)} \sim 37$ K, which could be obtained with a magnetic field of 14 T. The transition upon cooling exhibits a two step behavior. The first step is characterized by kinetics effects in which the transition temperature is found to depend approximately to the logarithm of the temperature rate with coefficient -3.8 K. We have given an interpretation of the two steps and the kinetics in terms of Mn Bi order-disorder effects in the NiAs-type structure.

6 Acknowledgement

This work has been partially performed at NanoFacility Piemonte, INRIM, a laboratory supported by Compagnia di San Paolo. The research leading to these results has received funding from the EC 7th Framework Programme

under grant agreement n.214864 (Project SSEEC).

References

Andersen, A., Halg, W., Fischer, P., Stoll, E., 1967. The magnetic and crystallographic properties of MnBi studied by neutron diffraction. Acta Chemia Scandinavica 21, 1543.

Basso, V., Beatrice, C., LoBue, M., Tiberto, P., Bertotti, G., 2000. Connection between hysteresis and thermal relaxation in magnetic materials. Phys. Rev. B 61, 1278.

Basso, V., Olivetti, E., Martino, L., Sasso, C., Kuepferling, M., 2012a. Entropy change at the magnetostructural phase transition of polycrystalline MnBi. In: Vasile-Muller, C., P.Egolf (Eds.), Refrigeration Science and Technology proceedings, IIR-IIF, N.2012-5. pp. 153–160.

Basso, V., Sasso, C. P., Skokov, K. P., Gufleisch, O., Khovaylo, V. V., 2012b. Hysteresis and magnetocaloric effect at the magnetostructural phase transition of Ni-Mn-Ga and Ni-Mn-Co-Sn Heusler alloys. Phys. Rev. B 85, 014430.

Bean, C. P., Rodbell, D. S., 1962. Magnetic disorder as a first-order phase transformation. Phys. Rev. 126, 104.

Chen, T., Stutius, E., 1974. The phase transformation and the physical properties of the MnBi and $Mn_{1.08}Bi$ compounds. IEEE Trans. Magn. 10, 581.

Coey, J. M. D., 2009. Magnetism and magnetic materials. Cambridge University Press, Cambridge.

Heikes, R. R., 1955. Magnetic transformations on MnBi. Phys. Rev. 99, 446.

Hubermann, B. A., Streifer, W., 1975. Coupled order paramaters, lattice disorder, and magnetic phase transitions. Phys. Rev. B 12, 2741.

Roberts, B. W., 1956. Neutron diffraction study of the structures and magnetic

properties of manganese bismuthide. Phys. Rev. 104, 607.

Yang, J. B., Yelon, W. B., James, W. J., Cai, Q., Kornecki, M., Roy, S., Ali, N., lHeritier, P., 2002. Crystal structure, magnetic properties and electronic structure of the MnBi intermetallic compound. J. Phys.: Condens. Matter 14, 6509.

Yin, F., Gu, N., Shigematsu, T., Nakanishi, N., 1996. Sintering formation of low temperature phase MnBi and its disordering in mechanical milling. J. Mater. Sci. Technol. 12, 335.

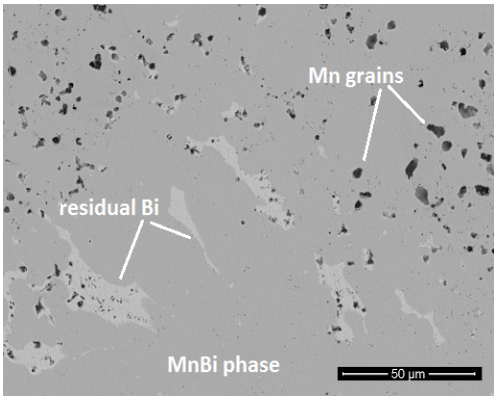

Fig. 1. SEM Back-scattered electrons image of the annealed sample polished surface. The three phases with different average atomic numbers appear with different gray levels.

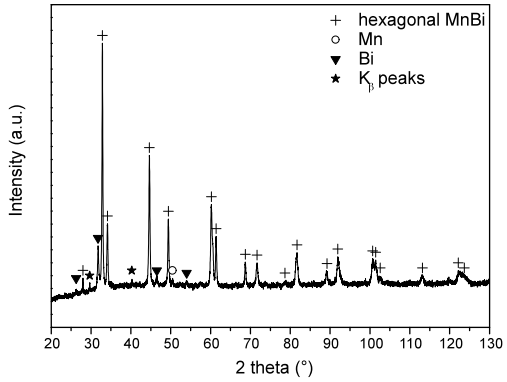

Fig. 2. XRD pattern of the studied alloy, square root of experimental intensity is displayed for better evaluation of the weaker reflections.

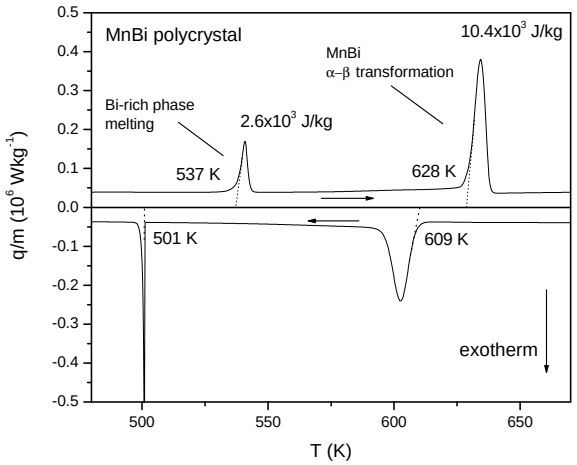

Fig. 3. Mass specific heat flux from DSC at the temperature rate of 0.167 Ks^{-1} (10 K/min).

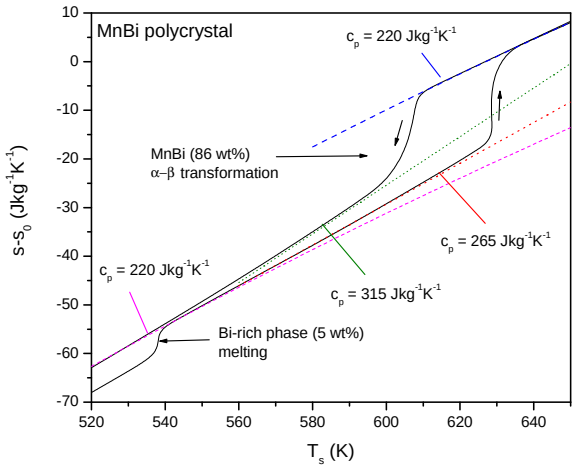

Fig. 4. Specific entropy computed from the heat flux of Fig.3. The reference value s_0 is the entropy of the paramagnetic state at 628 K.

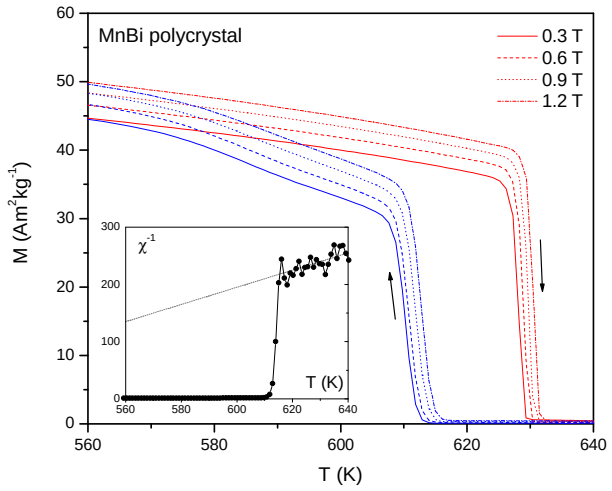

Fig. 5. Magnetization as a function of temperature measured by VSM. Temperature scan rate is 0.027 Ks^{-1} (1.6 K/min). The inset shows the inverse susceptibility on cooling from the same data.

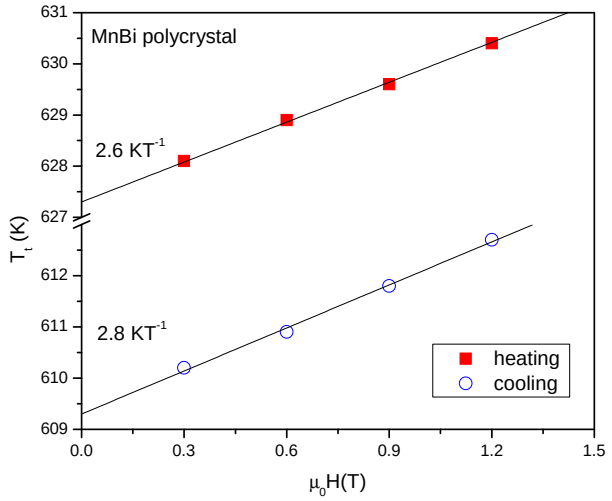

Fig. 6. Transition temperatures as a function of the applied magnetic field on both heating and cooling (from the data of Fig.5).

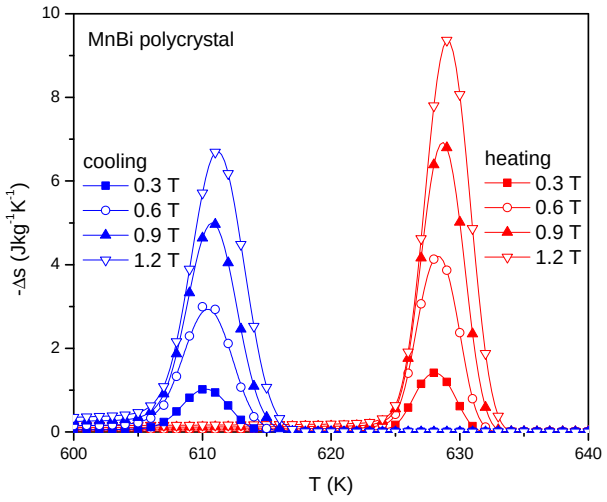

Fig. 7. Magnetic field induced entropy change computed by the Maxwell relation from the data of Fig.5. Heating and cooling branches were analyzed separately.

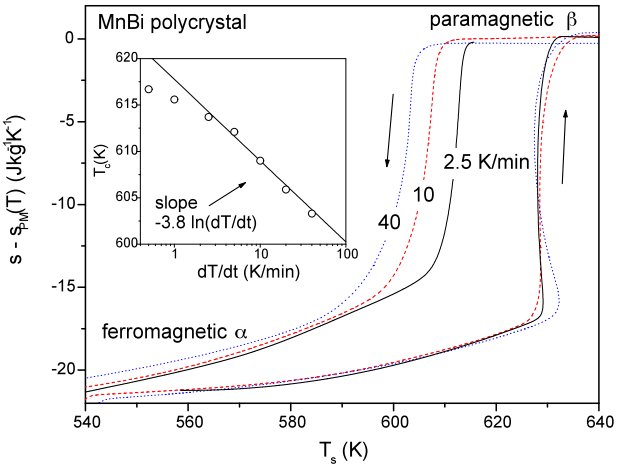

Fig. 8. Entropy diagram for the MnBi polycrystal under different temperature rates. The inset shown the transition temperature upon cooling.

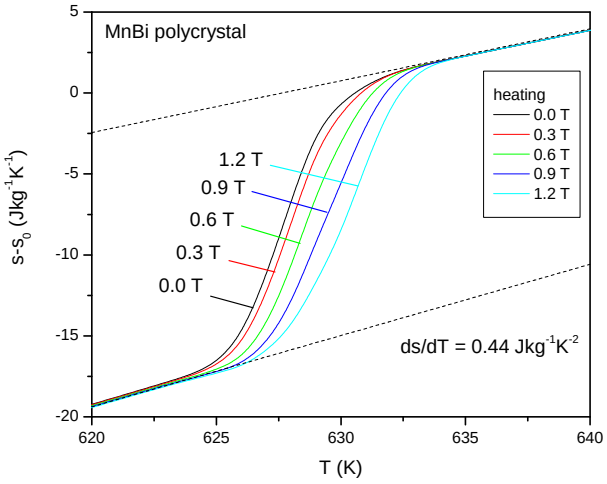

Fig. 9. Entropy diagram for the MnBi polycrystal (only heating curves are shown). The 0.0 T curve is obtained by a DSC thermal measurement. The curves under magnetic field are computed (Eq.4) by adding the magnetic Δs data of Fig.7

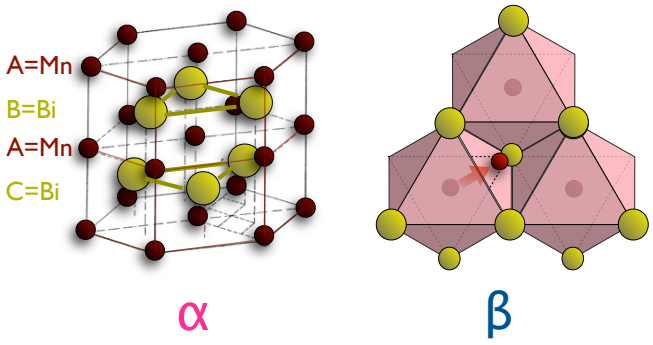

Fig. 10. Left: elementary NiAs-type cell of the α MnBi. Right: diffusion of a Mn atom from an octahedral site (α phase) to a trigonal bipyramidal hole (β phase).